PSFC/RR-03-9

The Zeeman effect on the n=7-6 and n=6-5 lines of H-like B and its influence on CXRS measurements in the Alcator C-Mod tokamak.

Marr, K.M., Terry, J., Lipschultz, B.

Written in 2003, electronically published in 2010

Plasma Science and Fusion Center
Massachusetts Institute of Technology
Cambridge MA 02139 USA

This work was supported by the U.S. Department of Energy, Grant No. DE-FC02-99ER54512. Reproduction, translation, publication, use and disposal, in whole or in part, by or for the United States government is permitted.

The Zeeman Effect on the $n' = 7 \rightarrow n = 6$ and $n' = 6 \rightarrow n = 5$ lines of H-like B and its Influence on CXRS Measurements in the Alcator C-Mod Tokamak

Kenneth D. Marr, James Terry, Bruce Lipschultz

March 27, 2003

Abstract

Charge-exchange Recombination Spectroscopy (CXRS) is an important diagnostic tool for determining the ion temperatures and bulk flows in tokamak plasmas. However, in plasma devices with high magnetic fields, such as Alcator C-Mod, transition line splitting due to the Zeeman Effect can play an important role in the measured spectra. The Zeeman Effect widens lines in the emission the spectrum as well as shifts them in wavelength. Calculations of these effects (in the high-field limit) are presented here for two $n' \rightarrow n$ transitions arising from charge-exchange of neutral hydrogen with fully stripped boron. The primary transition considered is $n' = 7$ to $n = 6$ in H-like boron near 4945 Å. The $n' = 6$ to $n = 5$ transition in H-like boron near 2982 Åis also considered. We show the errors in the inferred ion temperature and rotation velocity that result if the Zeeman Effect is neglected and conclude that in Alcator C-Mod this effect should be deconvolved from an experimental spectrum to improve the accuracy of temperature measurements.

1 Charge-exchange Recombination

Two of the more important measurements for tokamak plasmas are the ion temperature profile and the radial profile of any bulk flow velocities in the plasma. One of the more common methods for measuring these quantities is to analyse the spectra produced when hydrogen or deuterium atoms from a neutral beam interact with low-Z ions that are intrinsic to the plasma. Some of the beam atoms charge-exchange with the fully-stripped ions, resulting in H-like ions in a highly excited states. These excited states relax radiatively via line emission. Thermal motion of the plasma ions results in Doppler-broadened emission lines, and any bulk motion of the ions along the line-of-sight results in Doppler shifts of the line centers from their rest wavelengths. Thus measurement of the line shape and a line's absolute wavelength provides the necessary data for calculating the impurity ion temperature and the component of its bulk flow along the line-of-sight. Presuming the low-Z ions are in thermal equilibrium with, and flow at the same speed as, the background plasma ions, the plasma ion temperature and flow are obtained.

We now briefly examine the population distribution of excited states in the H-like ion formed by charge-exchange recombination. It has been shown that an electron exchanged in this way tends

to preserve its original energy and radius.[3] This means an electron previously in the ground state around a hydrogen atom will settle into an excited n-level around an impurity ion with $Z > 1$ to preserve energy. For these high n transitions, conservation of angular momentum will preferentially drive the electrons into states with l approximately equal to n. It has theorized that this is a result of the large-impact-parameter or "soft" collisions stripping off electrons that are far from the hydrogen nucleus in eccentric orbits with large kinetic energies.[4] In this manner, the cross-sections for charge-exchange recombination tend to peak at high n, l, when the charge of the receiving ion is greater than $Z = 1$. For example, a charge-exchange from ground-state hydrogen to fully-stripped boron will have cross-sections that are peaked at $n = 4$, $l = 3$.[4] [2]

Although the cross-sections peak at $n = 4$ for charge-exchange with B^{+4}, the emission lines from this level occur in the ultraviolet, making measurement significantly more difficult than measurements using visible light. Therefore, the visible transition, $n' = 7 \rightarrow n = 6$ (4945 Å), and near UV transition, $n' = 6 \rightarrow n = 5$ (2982 Å), though less intense, are more likely to be used in an experiment and were selected for this analysis.

Because of the small energy difference between l-levels of a sufficiently high principle quantum number, n, the collisional excitation/decay rates between the l-levels can be much higher than the radiative decay rates. Thus, above some critical density[1] the l-level distribution will be statistically populated. That critical density for H-like levels is

$$n_i^{crit} \approx \frac{Z^6\sqrt{T_i} \times 10^{10}}{Z_{eff}} \mathrm{cm}^{-3},$$

where Z is the charge of the H-like ion, T_i is the ion temperature in keV, and Z_{eff} is the effective charge of the plasma ions.[2] For example, for $n = 4$ in H-like boron the critical density is approximately 8×10^{12} cm $^{-3}$ (at 100eV), a density well below typical C-Mod densities. Thus in C-Mod the l-levels are completely mixed and populated according to their statistical weights.

2 Relative Intensities of the Lines Within the Multiplet

The Zero-Field Limit The relative intensities of the individual lines that make up the $n' \rightarrow n$ multiplet play an important part in shaping the overall spectra. The relative intensities[2] for the $B_{ext} = 0$ case, or the so-called fine structure, are shown in Figure 1. The appropriate eigenstates in this case (and in the "low-field" case) are labelled by the principal quantum number, n; the orbital angular momentum quantum number, l; the total angular momentum quantum number, j; and the projections of the total angular momentum, m_j. (In the $B_{ext} = 0$ case the j levels are $2j + 1$ degenerate in m_j and thus $2j+1$ populated.) Because the sublevels are populated according to their statistical weights (see above), it follows that the relative intensity of a transition will be governed by the relative population of the upper state, and the probability that it will transition down.

$$I_{rel} = A_{upper \rightarrow lower} * N_{upper} \tag{1}$$

where A is Einstein's spontaneous emission coefficient for the transition and N is the population of the upper state. The populations and probabilities of transition are already known in the $B_{ext} = 0$

[1] To ensure sufficient probability for the occurance of collisions

[2] All graphs are shown for transitions in air

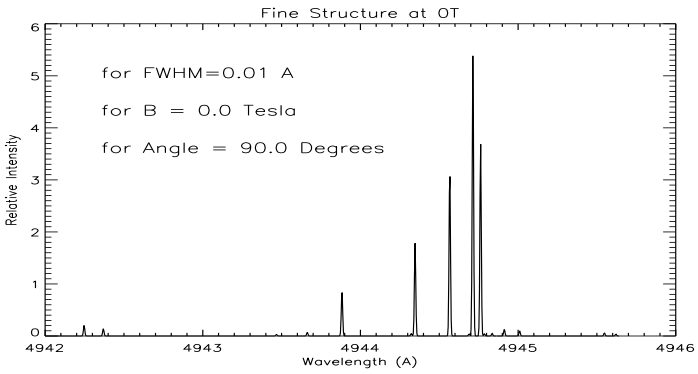

Figure 1: Fine spectrum for boron $n' = 7$ to $n = 6$

Table 1: **Most Prominent Fine Structure Transitions** $7 \rightarrow 6$

l'	j'	l	j	Wavelength (Å)	Relative Intensity	ζ (x10^{-5} eV)
6	6.5	5	5.5	4944.766	64.9	1.27
6	5.5	5	4.5	4944.717	58.4	1.27
5	5.5	4	4.5	4944.717	40.0	2.33
5	4.5	4	3.5	4944.570	32.6	2.33
4	4.5	3	3.5	4944.570	23.6	4.99
4	3.5	3	2.5	4944.350	18.2	4.99
3	3.5	2	2.5	4944.350	13.0	14.0
3	2.5	2	1.5	4943.885	9.10	14.0
2	2.5	1	1.5	4943.885	6.39	69.9
2	1.5	1	0.5	4942.248	3.56	69.9

Note that at 4T $\mu_B B \sim 23$ x10^{-5} eV

case:

$$I_{j' \rightarrow j} = (2j' + 1) * A_{j' \rightarrow j}$$

The transitions that contribute the most to the overall line shape are listed in Table 1.

The Zeeman Effect has typically been neglected as a significant factor in determining the measured line shapes [find refs] because in most tokamaks the charge-exchange lines-of-interest are emitted in magnetic fields lower than $\sim 3T$. Considering the fine-structure only had been sufficient in these "weak-field" cases. However, Alcator C-Mod operates routinely at on-axis fields of 5.4T, with the capability of fields up to 9.0T. The fields at the regions of emission then, range from 4.0T to 5.4T in the first case and from 6.7T to 9.0T in the second. Therefore, it is prudent when making measurements of this kind on C-Mod to examine the effects of the external magnetic field on the line shapes.

Table 2: **Most Prominent Combined Zeeman Effected Lines at 4T**

Wavelength (Å)	Relative Intensity
4943.964	0.0667
4944.263	0.5136
4944.477	0.1259
4944.719	1.0000
4945.174	0.4889

The Zeeman Effect We digress for a moment to discuss the Zeeman Effect in the high-field limit. The effects of an external magnetic field will differ depending upon the relative strength of the external field compared to that of the field internal to the atom or ion (the spin-orbit interaction). We can characterize the magnitude of the energy shift due to internal fields, a.k.a. the spin-orbit interaction or fine structure, by the quantity ζ. We then find the weak-field case when $\mu_B B_{ext} < \zeta$, where internal effects dominate the splitting. The high-field limit is such that $\mu_B B_{ext} > \zeta$ and external sources define the magnitude of the splitting. Assuming the central field caused by the hydrogenic ion is purely Coulombic,[3] ζ is given by

$$\zeta = \frac{\hbar^2 Z^4 e^2}{2m_0^2 c^2 a_0^3 n^3 l(l+1/2)(l+1)}\text{eV}. \tag{2}$$

The quantity ζ is related to the energy splitting in the fine structure as

$$\Delta E = \frac{1}{2}\zeta\left\{j(j+1) - l(l+1) - s(s+1)\right\}.[1] \tag{3}$$

If the energy shifts are already documented, as is the case for $B_{ext} = 0$, ζ can be more easily evaluated for different j levels using Equation (3) solved for ζ.[6]

The last column in Table 1 lists the value of ζ for all the transitions that compose the main lines of the fine structure. Recall that at 4T, $\mu_B B_{ext} \sim 23$ x 10^{-5} eV. Comparing this value to those found in Table 1, it is seen that except for the lowest transitions which are almost a factor of ten smaller than the peak, $\mu_B B_{ext}/\zeta > 1$. Thus for magnetic fields above approximately 4 Tesla the high-field limit applies to the transitions that are of interest on C-Mod. The consequence of this is that the spin decouples from the orbital angular momentum and the quantum numbers j and m_j no longer have meaning. Instead, for these hydrogen-like transitions, the appropriate quantum states[4] are labelled by the separate angular momentum and spin projections, n, l, m_l, m_s.

The Strong-Field Limit We desire to calculate the intensities and wavelengths of the transitions for the $n' = 7 \rightarrow n = 6$ and the $n' = 6 \rightarrow n = 5$ multiplets of BV under the influence of an external magnetic field in the high field limit. In order to calculate these intensities we must consider the quantum mechanical probability for emission from a radiating electric dipole for various polarizations.

[3] See further [1] pg 63,129.

[4] The quantum label of total spin, S, will be implied as we only deal with fermions

The polarization that a particular transition within the multiplet will aquire is dependent on its selection rule. $m_l' = m_l$, $m_l' = m_l + 1$, and $m_l' = m_l - 1$ will transition with linear, left circular, and right circular polarization respectively.[5] For simplicity, we still group transitions by their selection rule and include viewing angle factors in our intensity calculation. The emissivity per steradian is given by

$$\begin{array}{lcll} I_{n'l',m_l',m_s\to n,l,m_l,m_s} & \propto & \frac{1}{4\pi}\sin^2\theta A_{n'l',m_l',m_s\to n,l,m_l,m_s}N_{n'l',m_l',m_s} & \text{for} \quad m_l' = m_l \\ I_{n'l',m_l',m_s\to n,l,m_l,m_s} & \propto & \frac{1}{8\pi}(1+\cos^2\theta)A_{n'l',m_l',m_s\to n,l,m_l,m_s}N_{n'l',m_l',m_s} & \text{for} \quad m_l' = m_l + 1 \\ I_{n'l',m_l',m_s\to n,l,m_l,m_s} & \propto & \frac{1}{8\pi}(1+\cos^2\theta)A_{n'l',m_l',m_s\to n,l,m_l,m_s}N_{n'l',m_l',m_s} & \text{for} \quad m_l' = m_l - 1 \end{array} \tag{4}$$

Again we see that the emissivity is dependent upon the transition probability, A, and the population of the upper state, N.[5]

However, because we are not familiar with the transition statistics for any particular transition within a multiplet, we must turn to another method of calulation for the emission probability. We may use the quantum mechanical matrix elements for polarized emission to calculate these emission probabilities. These matrix elements fortunately have simple solutions given an appropriate choice of coordinate system. The polarization coordinates most commensurate with this problem is that of spherical tensor components: linear ($\hat{\mathbf{z}}$), left circular ($\mathbf{e_{+1}}$), and right circular ($\mathbf{e_{-1}}$). A line-of-sight ray would make an angle θ with the magnetic field and be expressed as:

$$\begin{array}{lcl} \mathbf{r} & = & r_0\hat{\mathbf{z}} + r_{+1}\mathbf{e_{+1}} + r_{-1}\mathbf{e_{-1}} \\ r_{\pm 1} & = & \frac{1}{\sqrt{2}}(x \pm iy) \end{array} \tag{5}$$

where we have defined $\hat{\mathbf{z}}$ by the direction of the external magnetic field and restricted propagation to the $\hat{\mathbf{x}} - \hat{\mathbf{z}}$ plane, that is, in the real part of $\mathbf{r}$.[1] The non-zero matrix elements grouped by their l-level transition may then be presented as:

$$\begin{array}{lrcl} l' = l + 1 & & & \\ & |< n', l+1, m_l, m_s|r_0|n, l, m_l, m_s >|^2 & = & \left\{(l+1)^2 - m_l^2\right\}\alpha \\ & |< n', l+1, m_l+1, m_s|r_{+1}|n, l, m_l, m_s >|^2 & = & \frac{1}{2}(l+m_l+1)(l+m_l+2)\alpha \\ & |< n', l+1, m_l-1, m_s|r_{-1}|n, l, m_l, m_s >|^2 & = & \frac{1}{2}(l-m_l+1)(l-m_l+2)\alpha \\ \text{with} & \Sigma_{m_l'}|< n', l+1, m_l', m_s|\mathbf{r}|n, l, m_l, m_s >|^2 & = & (l+1)(2l+3)\alpha \\ l' = l - 1 & & & \\ & |< n', l-1, m_l, m_s|r_0|n, l, m_l, m_s >|^2 & = & \left\{l^2 - m_l^2\right\}\beta \\ & |< n', l-1, m_l+1, m_s|r_{+1}|n, l, m_l, m_s >|^2 & = & \frac{1}{2}(l-m_l)(l-m_l-1)\beta \\ & |< n', l-1, m_l-1, m_s|r_{-1}|n, l, m_l, m_s >|^2 & = & \frac{1}{2}(l+m_l)(l+m_l-1)\beta \\ \text{with} & \Sigma_{m_l'}|< n', l-1, m_l', m_s|\mathbf{r}|n, l, m_l, m_s >|^2 & = & l(2l-1)\beta \end{array} \tag{6}$$

These equations are valid for both the strong and weak field limits,[5] using the respective good quantum numbers, and are shown here in the strong-field limit.[1] To complete our calucations we must discover the coefficients α and β.

[5]For one electron systems. $j' = j$ not shown as it only applies to weak transitions.

The calculation of these coefficients is easily accomplished if one notes that for any field strength n, l are still good quantum numbers. It follows from Equation (1) that the following are equal:

$$\begin{gathered} A_{n',l'\to n,l} N_{n',l'} = \Sigma_{j',j} A_{n',l',j'\to n,l,j} N_{n',l',j'} = \\ I_{n',l'\to n,l} = \Sigma_{j',m'_j,j,m_j} I_{n',l',j',m'_j\to n,l,j,m_j} = \Sigma_{m'_l,m'_s,m_l,m_s} I_{n',l',m'_l,m'_s\to n,l,m_l,m_s} \end{gathered} \tag{7}$$

This equality allows the calculation of the coefficients by using appropriate sums of zero-field intensities (the right term in the top half of the equality), calculated previously, and the last equation in each grouping of equations (proportional[6] to right most term in the bottom half of the equality). This reduces the calculation of α and β to simple arithmetic, solely dependent on the particular n', l', n, l levels and the zero-field transition intensities restricted to them. Explicitly this relation for a given $n', l' \to n, l$ is

$$\begin{array}{lcll} \Sigma_{j',j}(2j'+1)A_{j'\to j} & = & 2*(l+1)(2l+3)\alpha & \text{for} \quad l' = l+1 \\ \Sigma_{j',j}(2j'+1)A_{j'\to j} & = & 2*l(2l-1)\beta & \text{for} \quad l' = l-1 \end{array} \tag{8}$$

Once the matrix elements have been obtained they can be used in the equations that incorporate the specific geometry of observation relative to the external magnetic field direction. Again we will group the allowed transitions into the two cases based on the selection rules. Namely $\Delta m_l = 0$ (or π polarization) and $\Delta m_l = \pm 1$ (or σ polarization). In π polarization the emitted electric field is parallel with the external magnetic field whereas in σ polarization it lies in the plane perpendicular to the magnetic field.[1] The individual equations for the relative intensities with this grouping are:

$$\begin{array}{lll} \pi & \Delta m_l = 0 & \sin^2\theta \,|< n', l', m_l, m_s | r_0 | n, l, m_l, m_s >|^2 \\ \sigma & \Delta m_l = +1 & \frac{1}{2}(1+\cos^2\theta)\,|< n', l', m_l+1, m_s | r_{+1} | n, l, m_l, m_s >|^2 \\ & \Delta m_l = -1 & \frac{1}{2}(1+\cos^2\theta)\,|< n', l', m_l-1, m_s | r_{-1} | n, l, m_l, m_s >|^2 \end{array} \tag{9}$$

It can be seen that under transverse observation the σ polarization retains the extra factor of $\frac{1}{2}$ for its relative intensity. This factor does not occur for longitudinal observation, allowing the total summed intensity to remain constant. Table 2 lists the four most important transition values for the boron spectra when considering the Zeeman Effect at 4T.

Alcator C-Mod The viewing geometry on Alcator C-Mod is shown schematically for two characteristic views; one to measure primarily toroidal motion and the other to measure primarily poloidal motion. With regard to magnetic fields in the device, the poloidal observation is approximately transverse, while the toroidal one is essentially longitudinal.

A spectrum showing the effect of a 4T field on the $n' = 7 \to n = 6$ lines of H-like B in transverse observation are shown in Figure 2. Note the tendency toward a typical Zeeman "triplet" of relative intensity 1:2:1. As the field strength is raised the spectrum even more closely resembles a "triplet".

3 Wavelengths of the Lines Within The Multiplet

The Zero-Field Limit It is well known that the total energy difference between levels in a transition, ΔE, dictates the wavelength, λ, of the emission. For electromagnetic radiation in a

[6] The sum over m_s gives the factor of 2 found in Equation (8)

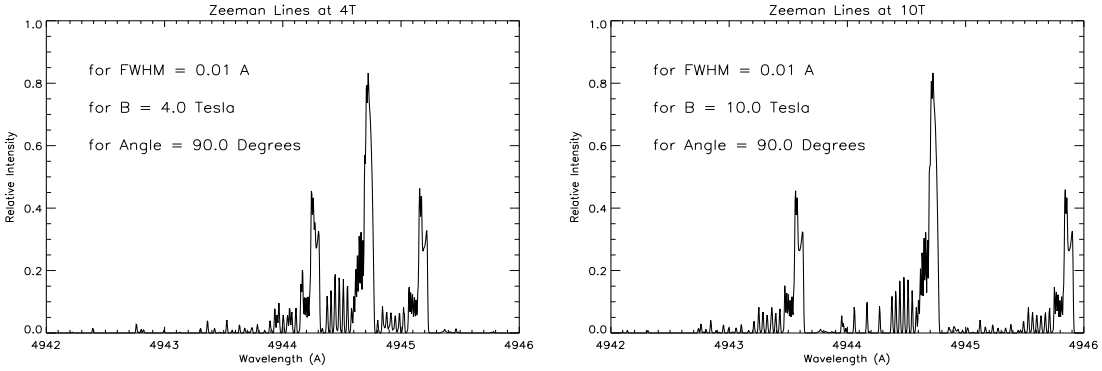

Figure 2: Highly Resolved View of Transition $n' = 7 \rightarrow n = 6$ at 4T and 10T

vacuum:

$$\lambda = \frac{hc}{\Delta E} = \frac{hc}{h\nu} \tag{10}$$

Because the measurements are taken in air, in the analysis we simply multiply by the index of refraction in air for the appropriate wavelength.[7] The so-called fine-splitting of the energy levels of a hydrogenic atom in no external magnetic field, $B_{ext} = 0$, is fairly simple to calculate. The levels can be extrapolated from the levels in a hydrogen atom, compensating for a larger nucleus.[8] Again, this fine-structure spectra can be seen in Figure 1 for the $n' = 7 \rightarrow n = 6$ multiplet of BV in air and the wavelength values found in the fifth column of Table 1.

The High-Field Limit The energy splitting in a strong magnetic field is a different matter altogether. As the external field is increased all energy levels will begin to deviate from their original value, and eventually some energy levels will meet at similar values. This combining of energy levels is another indication of the strong field limit. These new energy levels dictate that an entirely new set of transitions and even new transition rules will be evident. The wavelengths of the new transitions will be dependent on the strength of the magnetic field as well as the internal value, ζ. The energy of a state will be perturbed according to the following relation:

$$\Delta E = (m_l + g_s m_s)\mu_B B_{ext} + \zeta m_l m_s \tag{11}$$

where g_s is the Dirac spin g-factor[9] ($\sim$2 for electron spin), and with $\mu_B B_{ext}$ and ζ defined as before. Therefore the energy difference of a transition is going to be perturbed by the increase of the upper state minus the increase of the lower state.

$$\Delta E_{trans} = \Delta E_{upper} - \Delta E_{lower} = \mu_B B \Delta m_l + \{\zeta' m_s m_l' - \zeta m_s m_l\}$$

Adding this energy shift to Equation (10) the shifted wavelength is found to be at:

[7] At STP and 4942 Å, $n_{air} = 1.0002791$

[8] The levels for many different atoms can also be found in [6]

[9] See further [1]

$$\lambda_s = \frac{hc}{\Delta E_0 + \mu_B B \Delta m_l + \{\zeta' m_s m_l' - \zeta m_s m_l\}} \tag{12}$$

where ΔE_0 is the unperturbed energy difference. As before, consideration must be taken for wavelengths calculated for measurements in air.[1]

4 Reducing the Error

For all the calculations in this research the instrumental spectrum will be assumed to have a resolution of 1-2 Åand be extremely well characterized. Also, all the lines will be assumed to have thermally widened into gaussians.

As an intermediate check we prepared graphs evidencing and reinforcing the need for accounting for Zeeman splitting. Figure 3 shows, in dashed lines, the Zeeman Effect for 10T, higher than the fields expected for C-Mod. These broad spectra were generated by convolving the instrumental spectrum (a gaussian with 1.8 Åat FWHM) with gaussians widened from thermal effects of the ions, centered at each transition wavelength and restricted to the relative intensities calculated above. Similarly the dash and dots line shows the effect at 4T. The solid lines represent the result if the effect were neglected and the transitions from the fine structure were used. The two sets of plots are for ions at 100eV and 1000eV and are normalized to have similar peak intensities. Also, at the bottom of the first plot in Figure 3 are the individual lines that comprise the fine structure at zero field. The second plot contains the high-field spectra but at high resolution. It can clearly be seen that there is significant difference in the FWHM of the spectra as well as a noticeable shift in the wavelength of the peak value.[10] At 4T this difference is lessened, but still apparent. As the temperature of the ions increases the error in temperature decreases for any field strength, as expected, and the error in velocity increases.[11]

Clearly a factor in the shape of the spectra, the Zeeman Effect must be accounted for in a proper determination of the ion temperature. To this end a program was created to fit multiple gaussians to the spectrum with only the overall shift, overall intensity, and an overall widening factor left to be determined. In the same manner that the normalized spectra was generated, the gaussians used in analysis will be centered on either the lines from the fine structure spectra or those calculated considering the Zeeman Effect. The program assumes a priori knowledge of the strength of the magnetic field. This program performed admirably upon test spectra, even when the data wavelength spacing was increased to simulate a lack of data within the instrumental width.

To quantify the error of neglecting Zeeman we ran this program upon multiple artificially created test spectra. In Figure 4 we see the results of this procedure. The initial spectra were generated as before, assuming a field strength of 4T and then deconstructed using the program at 0T (and 4T as a control model). The program utilizing a field strength of 4T accurately reproduced the initial parameters with only slight errors in the velocity at the highest temperatures. Utilizing 0T however, there was noticeable error in ion temperature (50% at 50 eV), that reduced with increasing

[10] Most easily seen by comparing relative position of Zeeman shifted wings near the half maximum in relation to the zero-field ones

[11] The increasing Doppler widening will wash out the thermal error of neglecting the intrinsic change in transition spectra

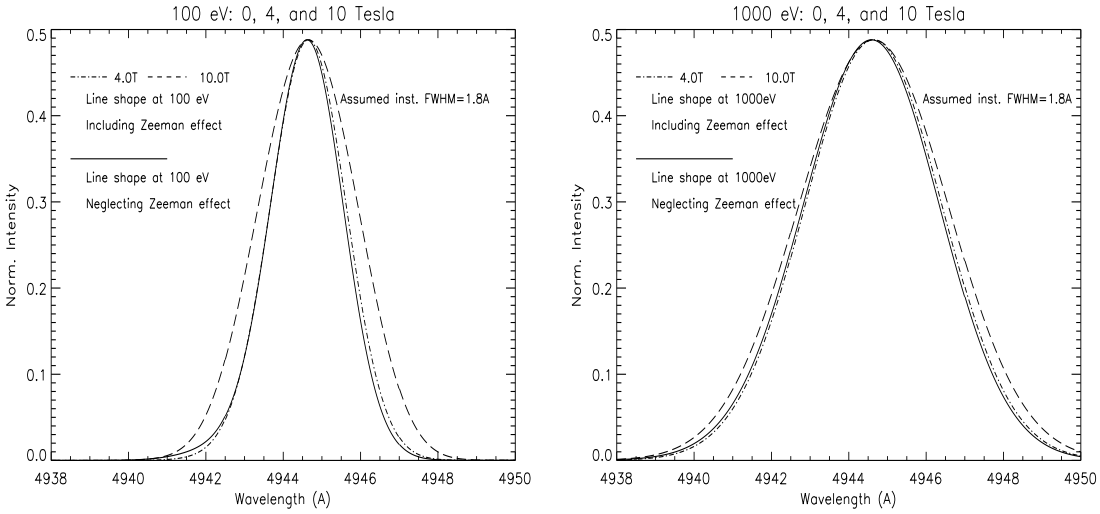

Figure 3: Normalized Spectra at Varying Temperatures and Magnetic Fields

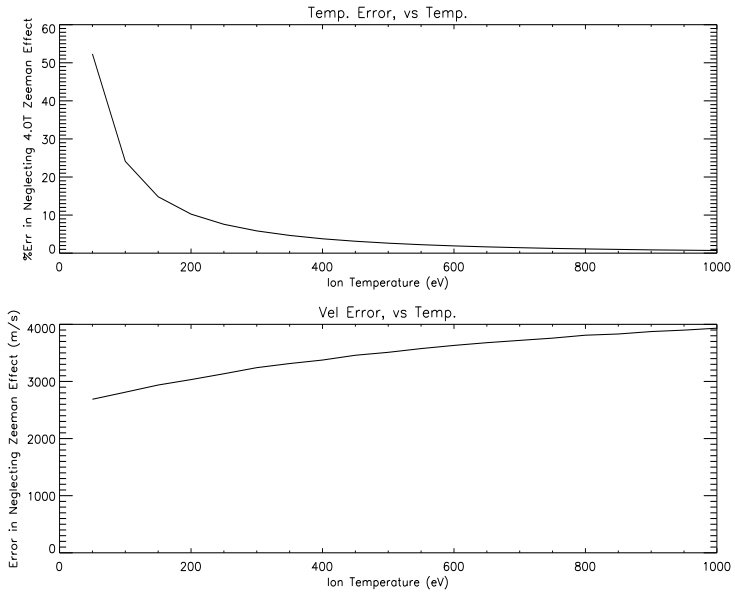

Figure 4: Percent Error in Temperature and Error in Bulk Velocity at 4T

temperature as expected. There was significant error in the bulk velocity, however, due to the inherent difference in peak wavelengths between the fine structure and the Zeeman Effect (∼3000 km/s. See peak intensities in Tables 1 and 2.) When the field strength of the test spectrum was increased to 10T, the neglect error in temperature increased significantly becoming almost 600% for 50eV. There was some increase in error for velocity, but it was much less significant.

Convinced of the need to account for the Zeeman effect, we proceeded to develop a simulated spectrum similiar to one expected from the spectrometer. Some of the complications added at this point were electronic (or dark) noise from the CCD, noise due to photon statistics, a background level or continuum from temperature considerations on the device, even less data points, and a nearby BII line at 4940.38 Å. With the addition of each complication the fitting routine evolved to properly handle the modified spectra. Once a spectrum fully comparable with an experimental one was obtained, the fitting program was tested for its range and accuracy; both were satisfactory.

5 Concurrent Work by Colleagues in the Field

Parametrization of the Zeeman Effect The existence of the polarization triplet was recently used by Blom and Jupén as an alternate method for calculating the temperature of a plasma over a wide range of temperatures. A few key features of the triplet were used to derive three parameters based only on atomic structure. The polarization factors are combined into a relation between the π and σ intensities, namely

$$\frac{I_\pi}{I_\sigma} = \frac{2\sin^2\theta}{1+\cos^2\theta}.$$

This relation will be used in our C-Mod specific procedure to account for angle of viewing. The separation of the two smaller peaks is found to be linearly dependent on the magnetic field with scale factor α. The ratio of the widening effect by Zeeman to that of Doppler was found to be almost purely temperature dependent, with scale factor β and degree γ. These three parameters are only dependent on the transition in question and can be used in a program to fit three gaussians to a spectrum. In this way the temperature is found with significantly less error than totally neglecting the Zeeman Effect. Blom and Jupén calculated these values from experiment for many common transitions. Although less easily generalized to other transitions, we have found our procedure to be marginally more accurate for the transitions considered here. Many find that the procedure delineated by Blom and Jupén sufficient for their needs.

TOTALB Another method for analyzing the effects of plasma conditions on line width is being developed by Mark Adams, et al, in collaboration with the MIT Plasma Science and Fusion Center and researchers at CalTech. This program takes plasma parameters, such as density and temperature, and calculates the expected line width accounting for many effects, including Stark and Zeeman broadening. At printing the complete mathematical solution was beyond reasonable scope of computing powers, but methods for simplifications were available. Assuming they were not oversimplified, these methods showed that the Zeeman Effect would dominate other effects, such as Stark broadening, at the magnetic strengths desired. We eagerly await further development of this tool to compliment our procedure of spectral analysis.

6 Conclusions

With the development of newer fusion devices able to support stronger magnetic fields, it has become increasingly apparent that there is a need to account for magnetic field effects during diagnostics. FIRE for example, could run approximately at 7.8T at the edge. Alcator C-Mod is capable of performing consistently with fields up to 6.0T at the edge. It is imperative then that the Zeeman Effect be considered when accurately analyzing any charge-exchange recombination spectra at these fields. The error in measured ion temperature is greater at lower temperatures, but increases with magnetic field. The error in bulk velocity increases slightly with temperature and magnetic field, but is inherently significant, as mentioned above. With proper consideration, however, more accurate values for these variables can be obtained from experimental spectrum.

References

[1] Woodgate, G. *Elementary Atomic Structure.* McGraw-Hill Publishing Co. Ltd.. London, 1970

[2] Fonck, R., Darrow, D., and Jaehnig, K. *Determination of Plasma-Ion Velocity Distribution Via Charge-Exchange Recombination Spectroscopy.* Physical Review A **29** 6. (1984) 3288-3309.

[3] Olson, R. *Ion-Rydberg Atom Collision Cross Sections.* J. Phys. B: Atomic and Molecular Physics, **13**. (1980) 483-492.

[4] Olson, R. n, l *Distributions In* A^{q+}+ *H Electron-Capture Collisions.* Physical Review A, **24** 4. (1981) 1726-1733.

[5] ADAS603. *Zeeman multiplet line fitting.*

[6] Garcia, J. and Mack, J. *Energy Level and Line Tables for One-Electron atomic Spectra.* J. Optical Soc. of America **55** 6. (1964) 654+